PAPER • OPEN ACCESS

Identifying carbon emission reduction potentials of BIPV in high-density cities in Southeast Asia

To cite this article: Gabriel Happle *et al* 2019 *J. Phys.: Conf. Ser.* **1343** 012077

Identifying carbon emission reduction potentials of BIPV in high-density cities in Southeast Asia

Gabriel Happle[1,2], Zhongming Shi[1,2], Shanshan Hsieh[1,2,3], Bolie Ong[1], Jimeno A Fonseca[1,2] and Arno Schlueter[1,2]

[1] Future Cities Laboratory, Singapore-ETH Centre, 1 Create Way, Singapore 138602
[2] Architecture and Building Systems, Institute of Technology in Architecture, ETH Zurich, Stefano-Fanscini-Platz 1, CH-8093 Zurich, Switzerland
[3] Industrial Process and Energy Systems Engineering (IPESE), École Polytechnique Fédérale de Lausanne, CH-1950 Sion, Switzerland

E-mail: happle@arch.ethz.ch

Abstract. We use life cycle analysis, urban building energy simulations and urban form generation to compare the operational carbon emissions of buildings with building-integrated photovoltaics (BIPV) in locations with different grid electricity mixes in Southeast Asia. Our results show that BIPV installations can reduce operational carbon emissions of buildings by up to ∼50%. The entire roofs and ∼40-100% of the facades should be activated for solar energy harvesting, depending on the context and urban form. Additionally, we prove that it is more effective to install BIPV in countries with high carbon intensive grid electricity mixes, independent of climate and urban form.

1. Introduction

Studies of urban solar energy potential usually focus on the interplay of urban form with solar irradiation. When quantifying the potential solar energy yield and the resulting carbon emission reduction, two assumptions are often oversimplified. The first one is the selection of the building-integrated photovoltaics (BIPV) installation area. Usually, two cases are considered: Either the building envelope is covered entirely by BIPV, or the installation area is selected based on an annual solar irradiation threshold, e.g., 1000 $kWh_{sol}/m^2/yr$ [1]. This threshold usually limits the PV installation to roof surfaces. The second assumption is that each kWh of electricity harvested will reduce the operational carbon emissions of the district, i.e., the embodied carbon emissions of PV electricity are neglected [1].

In this article, we propose that the country-specific grid electricity mix limits the achievable urban solar energy potential. Figure 1 presents a comparison of the carbon emission intensity of different Southeast Asian grid electricity mixes and BIPV electricity produced under different annual solar irradiation values. The lower the solar irradiation onto the BIPV panels, the more carbon emissions from the life cycle of the panels are embodied in each kWh of electricity harvested. According to this reasoning, BIPV can be installed until the PV electricity reaches carbon emission parity with the grid, i.e., the "dirtier" the grid electricity mix is, the more BIPV can be installed to lower the operational carbon emissions of buildings. On the following pages, we present a method to quantify the interplay between urban form, urban solar energy potential, and carbon emission reduction on scenarios in Southeast Asia.

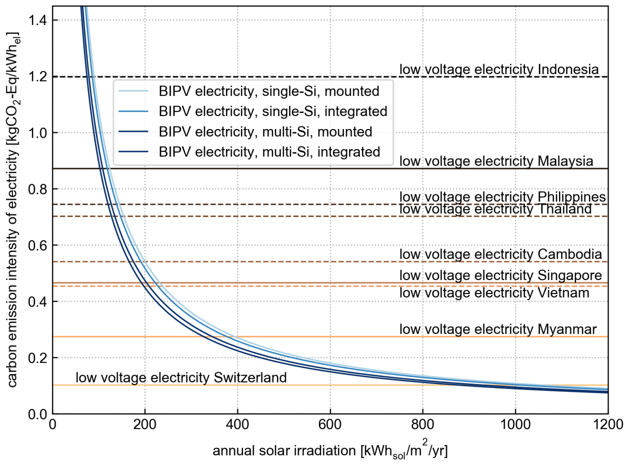

Figure 1. The carbon emission intensity of BIPV electricity for different annual solar irradiation values and the carbon emission intensity of different grid electricity mixes in Southeast Asia and Switzerland. The carbon emission intensity of BIPV electricity is calculated with Equation (1).

With this work we are aiming at answering the following research questions: Taking a local perspective, (1) what are the maximum operational carbon emission reductions and the corresponding urban solar energy penetrations in different countries?; (2) should building facades be activated to realize these carbon emission reductions? Taking a global perspective, (3) in which countries should BIPV be installed to reduce carbon emissions most effectively?

2. Method

2.1. Urban form generation

The urban form generation inherits the 13 types of block typologies made in a recent study on 178 blocks in six high-density mixed-use areas of Singapore [2]. They feature different floor area ratio (FAR, 3 to 10+), site coverage ratio (SCR, 0.4 to 1), and building patterns. The five types of building patterns featured include podiums, towers, podiums with towers, C-shape podiums, and shophouses. We randomly generate three districts using the block typologies in Grasshopper, see Figure 2. The random distributions intend to create various urban settings for the mutual shading of buildings in solar simulations.

2.2. Life cycle assessment

We use ecoinvent 3.5 [3] as the data source for the life cycle impact assessment (LCIA). We choose "Allocation, cut-off by classification" [4] as our system model and "IPCC 2013" [5] as our LCIA method to quantify climate change impacts with the indicator for 100-year global warming potential (GWP100a) in units of [kg CO_2-Eq], denoted as *carbon emissions* in this work. The impacts of the grid electricity mixes are taken from the market processes for low voltage electricity (see Figure 1). The impacts of the BIPV systems are extracted from the market processes for BIPV installations and normalized with the information of installation area, system lifetime and panel efficiency from [6]. For our analysis, we select the activity "photovoltaic facade installation, 3kWp, single-Si, laminated, integrated, at building" with carbon emissions of $Em_{BIPV} = 7240$ kg CO_2-Eq, which has an active surface $A_{BIPV} = 19.6$ m^2, a panel efficiency of $\eta_{BIPV} = 14\%$ and a system lifetime of $LT_{BIPV} = 30$ yr. Facade mounting systems, electric installations, inverters, and replacement of components are included. We use Equation (1) to calculate the carbon emission intensity $em_{BIPV}(I)$ of BIPV electricity harvested from a surface with annual solar irradiation I [kWh$_{sol}$/m^2/yr]. We assume a typical performance ratio for Singapore of $PR_{BIPV} = 0.85$ to account for various systems losses.

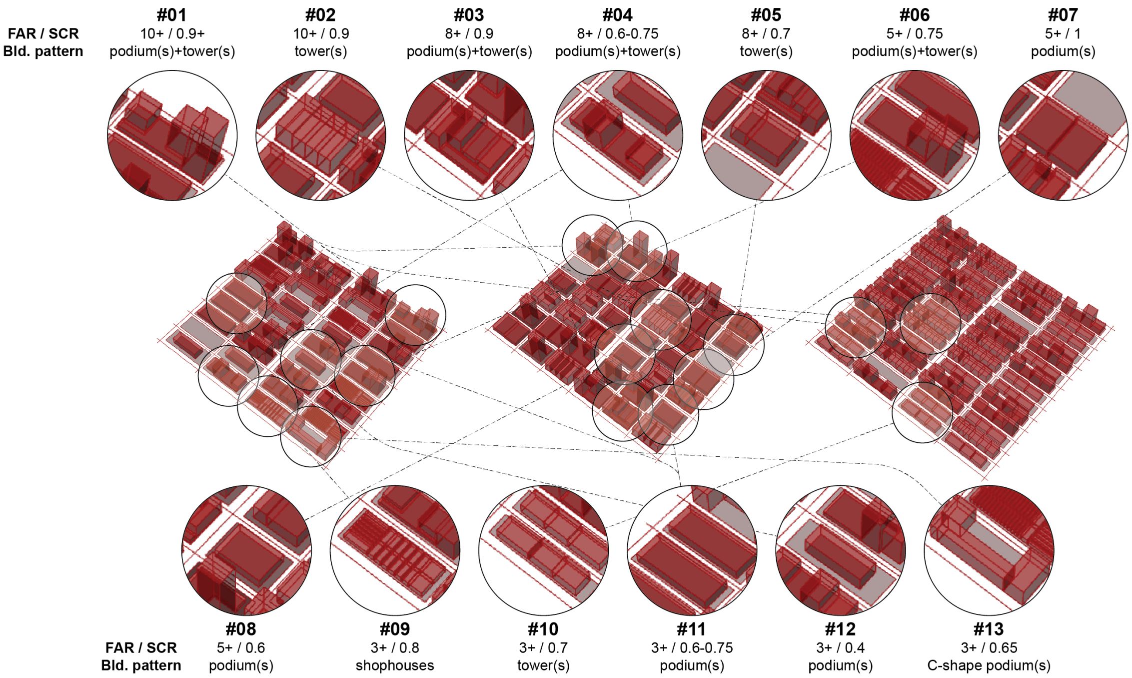

Figure 2. The three districts consist of the randomly distributed thirteen types (#01-#13) of block typologies.

$$em_{BIPV}(I) = \frac{Em_{BIPV}}{I * \eta_{BIPV} * PR_{BIPV} * A_{BIPV} * LT_{BIPV}} \quad [\text{kgCO}_2\text{-Eq/kWh}_{el}] \tag{1}$$

2.3. Urban energy simulation
An urban energy simulation toolbox, the City Energy Analyst (CEA) [7], is used to simulate the energy demand of the block typologies. For the solar radiation simulation, the CEA includes an interface to DAYSIM [8], which calculates the solar irradiation using a high-resolution virtual sensor grid covering the urban form. The output of the simulation includes the incremental envelope areas (A_i, i=1 . . . m) corresponding to the sensor grid and their annual solar irradiation. Construction and building system properties are equal in all simulations and based on typical values for Singapore as implemented in the databases of CEA. The thermal energy demands of buildings are supplied by electric systems. The buildings have a land use mix of 60% residential, 30% office, and 10% retail. The window-to-wall ratio is 0.29, leaving the major part of the facade available for potential BIPV installation. On the roof, panels are assumed to be integrated horizontally.

2.4. Operational carbon emission intensity of buildings and urban solar energy penetration
$em_b(n)$ is the operational carbon emission intensity of a building with BIPV installed on the surfaces with the highest annual solar irradiation until the n-th surface ($1 \leq n \leq m$). It is calculated with Equation (2), where $E_{BIPV,i} = I_i * \eta_{BIPV} * PR_{BIPV} * A_i$ [kWh$_{el}$/yr] is the annual PV energy yield of the incremental envelope surface A_i [m^2] receiving I_i [kWh$_{sol}$/m^2/yr] annual solar irradiation, GFA is the gross floor area of the building in [m^2], and em_G is the emission intensity of the respective grid electricity mix in [kgCO$_2$-Eq/kWh$_{el}$]. Urban solar energy penetration $sp(n)$ is calculated with Equation (3) as the fraction of cumulative annual BIPV yield of the total annual electricity demand E_D [kWh$_{el}$/yr].

$$em_b(n) = \frac{1}{GFA}(E_D * em_G - \sum_{i=1}^{n} E_{BIPV,i} * (em_G - em_{BIPV,i}(I_i))) \quad [\text{kgCO}_2\text{-Eq/m}^2_{GFA}/\text{yr}] \quad (2)$$

$$sp(n) = \frac{1}{E_D}\sum_{i=1}^{n} E_{BIPV,i} \quad [\text{-}] \quad (3)$$

2.5. Scenarios

We create four scenarios in total. The same districts are simulated using the country-specific grid electricity mix and the location-specific climate in Singapore, Johor Bahru (Malaysia) and Yangon (Myanmar). We calculate the fourth scenario (Singapore-CH) where Singapore has a hypothetical low carbon electricity supply, e.g., by importing hydropower or building a nuclear power plant. We use the Swiss grid electricity mix in this scenario. Singapore Downtown and Johor Bahru Downtown are only 25 km apart. However, the carbon emission intensity of their grid electricity mixes is very different. Singapore's electricity is mainly supplied by natural gas, while Malaysia's supply has a high share of coal power [9]. Myanmar has the "cleanest" electricity in the region due to its high share of hydropower in its mix [9]. We use the typical weather file for Singapore from [10], and for Johor Bahru and Yangon from [11].

3. Results

Figure 3 shows the interplay between operational carbon emission intensity and solar energy penetration for the different block typologies in the four scenarios. The markers indicate the minimum achievable operational carbon emission intensity and the corresponding optimal solar energy penetration for each block typology. The same markers with black edges are used to indicate the baseline condition without BIPV installed. For the condition of optimal solar energy penetration, Figure 4 shows the percentage of carbon emission reduction for each block typology, the average carbon emission reduction for every m^2 of BIPV installed, and the fractions of roof and facade covered by BIPV.

Installing BIPV in high-density urban settings is an effective way to decrease operational carbon emissions of buildings in all four scenarios. According to Figure 3 and Figure 4, urban solar energy penetrations in the range of ∼10% to ∼60%, result in operational carbon emission reductions from ∼3% to ∼50%. To achieve this in the Southeast Asian scenarios, the entire roof, and part of the facade (∼40%-100%) should be activated for solar energy harvesting. In the Singapore-CH scenario, there are no BIPV installations on the facade, and for some block typologies, the roof is not entirely activated. The slope of the curves in each scenario represents the effectiveness of BIPV as a means to reduce operational carbon emissions. Figure 4 shows that for each m^2 of BIPV installed in Malaysia up to 100 $kgCO_2$-Eq/yr will be reduced. The same installation in Singapore will reduce up to 50 $kgCO_2\text{-Eq/m}^2_{BIPV}$/yr. In Myanmar, it will reduce only 30 $kgCO_2\text{-Eq/m}^2_{BIPV}$/yr. From a global perspective, it is therefore much more impactful to install BIPV in contexts with higher carbon emission intensive grid electricity mixes.

In addition, we notice there are changes in the emission ranking of block typologies as the urban solar energy penetration increases, in Figure 3. From the perspective of urban design, we make three interpretations. Firstly, higher emission locations have a greater spread, meaning more sensitivity to the choice of block typology. Secondly, in each scenario, the best performing block typology depends on the targeted solar energy penetration. For example, block typologies with high densities (#01-#05) become less preferred at higher solar energy penetration. Finally, if a decision is made to build a sub-optimal block typology, a minimum BIPV installation shall be enforced to compensate for the higher emission intensity. For example, low-density block typologies like shophouses (#09) only outperform those with towers, if more than ∼35% solar energy penetration is attained.

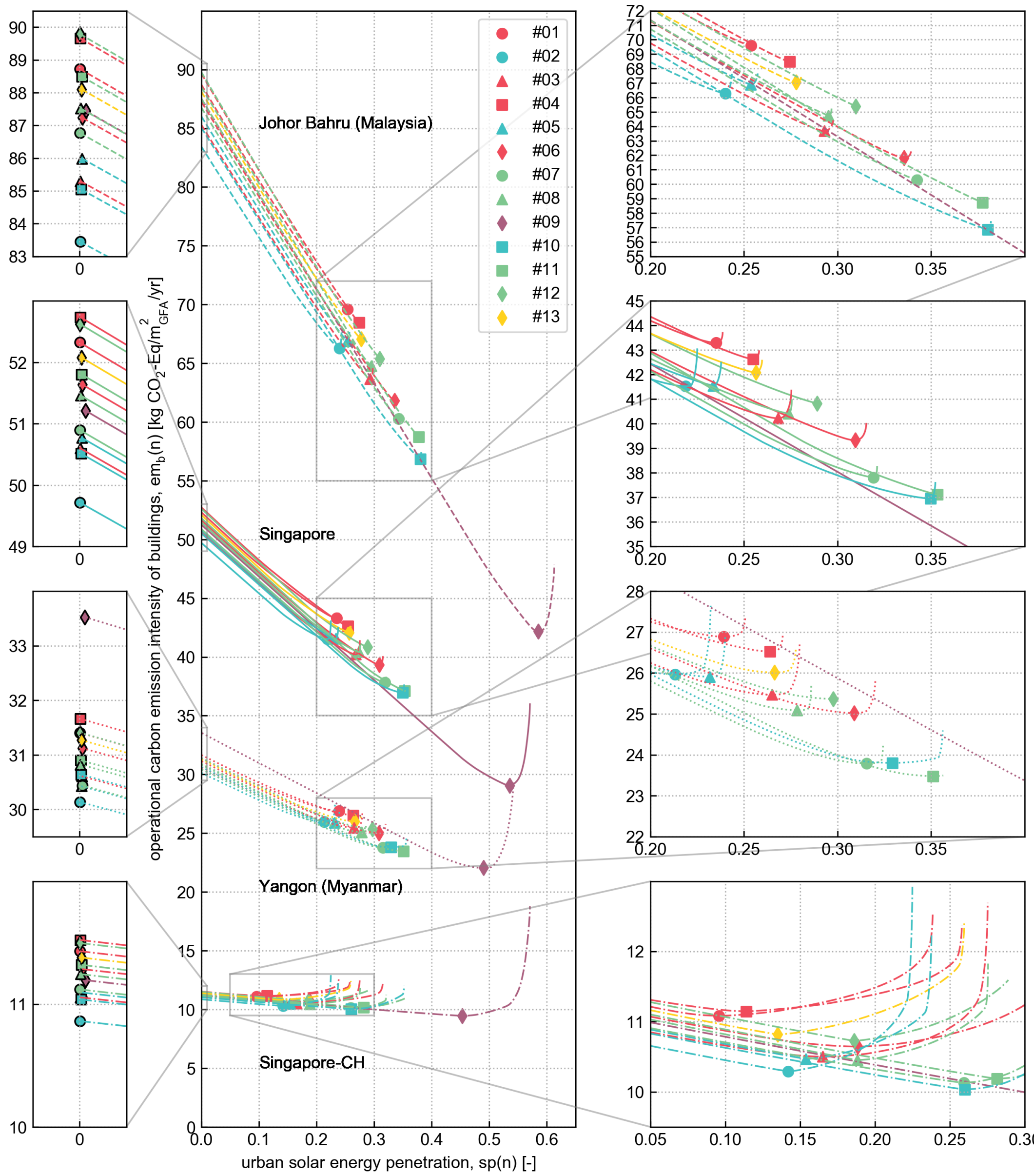

Figure 3. The relationship of operational carbon emissions of buildings to urban solar energy penetration for different block typologies in the four scenarios: - - - -Malaysia, ——Singapore, ······Myanmar, — · —Singapore-CH. Block typologies with the same building patterns share the same color: Podiums+towers (red), towers (blue), podiums (green), C-shape podiums (yellow), and shophouses (purple).

4. Conclusions and outlook

In this paper, we demonstrate that urban solar studies should not exclusively focus on the interplay of urban form and climate, but they should also consider the local context in the form of the grid electricity mix. Our results show that BIPV installation is a way to reduce carbon emissions in Southeast Asian cities by ∼15-50%. The entire roof and ∼40-100% of the facade of buildings should be activated for solar energy harvesting. More importantly, we prove that it is more effective to install BIPV in countries with high carbon intensive grid electricity mixes, independent of climate and urban form. Additionally, we can use this method to find insights

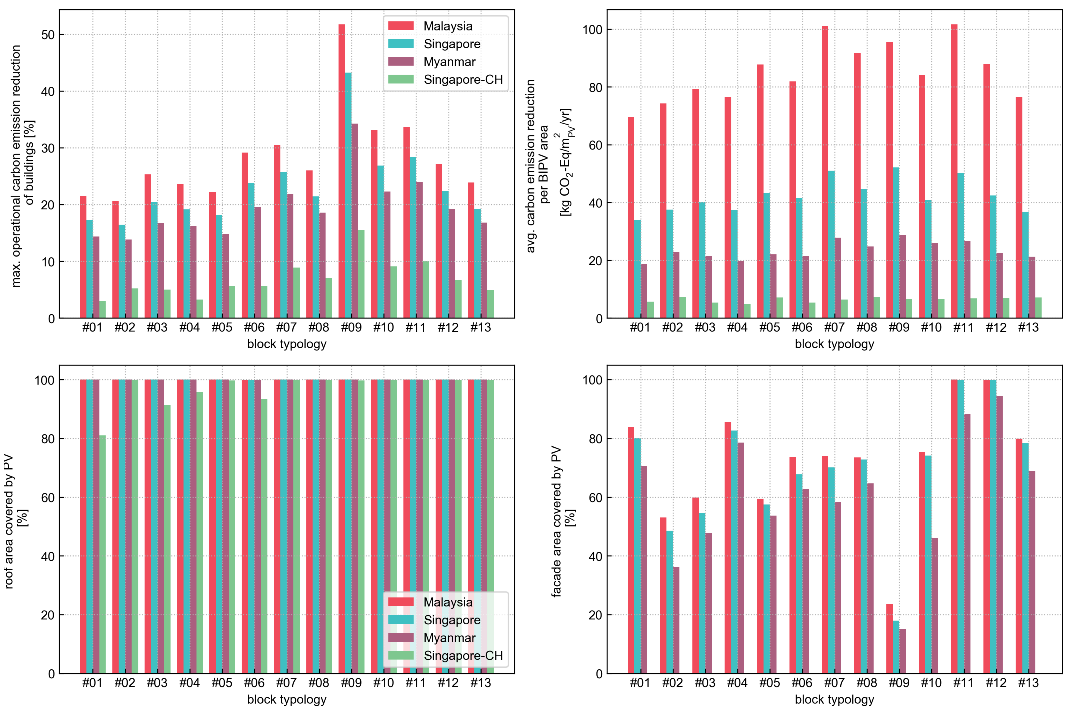

Figure 4. Maximum achievable operational carbon emission reductions of buildings (top left), emission reduction effectiveness of BIPV installation (top right), BIPV roof coverage (bottom left), and BIPV facade coverage (bottom right) for the block typologies in the four scenarios.

about the impacts of urban design on solar energy potential and carbon emission reduction. In the future, similar studies on energy economics should take the local cost structure of electricity prices and costs for BIPV installations into account, and other local and global life cycle impacts, like embodied energy, resource depletion, and ecotoxicity, should be included.

Acknowledgments

This work was developed at the Future Cities Laboratory at the Singapore-ETH Centre, which was established collaboratively between ETH Zurich and Singapore's National Research Foundation (FI 370074016) under its CREATE programme. We thank our colleague S Linsin.

References

[1] Zhang J, Xu L, Shabunko V, Tay S E R, Sun H, Lau S S Y and Reindl T **240** 513–533 ISSN 0306-2619
[2] Shi Z, Fonseca J A and Schlueter A Estimating the renewable energy potential with block typologies
[3] Wernet G, Bauer C, Steubing B, Reinhard J, Moreno-Ruiz E and Weidema B **21** 1218–1230 ISSN 1614-7502
[4] ecoinvent Association System Models in ecoinvent 3: Allocation cut-off by classification URL `https://www.ecoinvent.org/database/system-models-in-ecoinvent-3/cut-off-system-model/`
[5] IPCC 2013 Climate Change 2013: The Physical Science Basis. Contribution of Working Group I to the Fifth Assessment Report of the Intergovernmental Panel on Climate Change
[6] Jungbluth N, Stucki M, Flury K, Frischknecht R and Bsser S Life Cycle Inventories of Photovoltaics
[7] Thomas D, Fonseca J A, Sreepathi B K, Hsieh S, Mosteiro-Romero M, Happle G, Rogenhofer L, Khayatian F, Hawthorne J, Shi Z, Chen K, Ong B L, Neitzel P, Elesawy A, Acosta J A B and Marty V CityEnergyAnalyst v2.9.2 URL `https://zenodo.org/record/2553318`
[8] Reinhart C Daysim URL `https://daysim.ning.com/`
[9] IEA Statistics - Electricity generation by fuel URL `https://www.iea.org/statistics/`
[10] EnergyPlus Development Team Weather Data - EnergyPlus URL `https://energyplus.net/weather`
[11] Meteotest Meteronorm 7 URL `https://meteonorm.com/en/`